Assessing Footwear Effects from Principal Features of Plantar Loading during Running

MATTHIEU B. TRUDEAU, VINZENZ VON TSCHARNER, JORDYN VIENNEAU, STEFAN HOERZER, and BENNO M. NIGG

Human Performance Laboratory, Faculty of Kinesiology, University of Calgary, Calgary, Calgary, Alberta, CANADA

ABSTRACT

TRUDEAU, M. B., V. VON TSCHARNER, J. VIENNEAU, S. HOERZER, and B. M. NIGG. Assessing Footwear Effects from Principal Features of Plantar Loading during Running. *Med. Sci. Sports Exerc.*, Vol. 47, No. 9, pp. 1988–1996, 2015. **Purpose**: The effects of footwear on the musculoskeletal system are commonly assessed by interpreting the resultant force at the foot during the stance phase of running. However, this approach overlooks loading patterns across the entire foot. An alternative technique for assessing foot loading across different footwear conditions is possible using comprehensive analysis tools that extract different foot loading features, thus enhancing the functional interpretation of the differences across different interventions. The purpose of this article was to use pattern recognition techniques to develop and use a novel comprehensive method for assessing the effects of different footwear interventions on plantar loading. **Methods**: A principal component analysis was used to extract different loading features from the stance phase of running, and a support vector machine (SVM) was used to determine whether and how these loading features were different across three shoe conditions. **Results**: The results revealed distinct loading features at the foot during the stance phase of running. The loading features determined from the principal component analysis allowed successful classification of all three shoe conditions using the SVM. Several differences were found in the location and timing of the loading across each pairwise shoe comparison using the output from the SVM. **Conclusions**: The analysis approach proposed can successfully be used to compare different loading patterns with a much greater resolution than has been reported previously. This study has several important applications. One such application is that it would not be relevant for a user to select a shoe or for a manufacturer to alter a shoe's construction if the classification across shoe conditions would not have been significant. **Key Words:** RESULTANT FORCE, SHOES, PRINCIPAL COMPONENT ANALYSIS, SUPPORT VECTOR MACHINE, PATTERN RECOGNITION

The effects of different footwear on the musculoskeletal system are often assessed by interpreting the resultant ground reaction force acting at the foot during the stance phase of running. The heel impact peak and the loading rate are often extracted from the ground reaction force to make conclusions on the beneficial or harmful effects of different design features such as heel pad thickness, heel structure, or midsole material (2,7,8,19). However, the functional interpretation of results using these variables with respect to their beneficial or harmful effects on the musculoskeletal system is the subject of current debate in the literature (18). It may well be that additional kinetic information is required to develop better functional understanding of the effects that different footwear constructions have on the locomotor system. Measuring the loading patterns across the entire foot combined with pattern recognition analysis techniques provides potential for gaining relevant information that has previously been overlooked.

Plantar loading at the foot–shoe interface has been assessed as a measure of the loading applied to the body (4,5,8,23,24,26). Knowledge of the force magnitude and distribution under the entire foot is important because different plantar loading patterns have been shown to affect proprioceptive feedback (9,15,17). Altering plantar sensory feedback has been shown to affect the mechanics and movement patterns during gait (20). In fact, different pressure distribution patterns at the foot change the sensory input to the human body, which could be altered through footwear design to optimize comfort and improve perceptual motor performance (1,5,14,21). In addition, mediolateral pressure distributions reveal how different shoes may induce different lever arms and thus influence the stability of the foot (13).

Address for correspondence: Matthieu B. Trudeau, Ph.D., Human Performance Laboratory, University of Calgary, 2500 University Drive, Calgary, Alberta, T2N 1 N4, Canada; E-mail: mtrudeau@ucalgary.ca.
Submitted for publication October 2014.
Accepted for publication January 2015.
Supplemental digital content is available for this article. Direct URL citations appear in the printed text and are provided in the HTML and PDF versions of this article on the journal's Web site (www.acsm-msse.org).

0195-9131/15/4709-1988/0
MEDICINE & SCIENCE IN SPORTS & EXERCISE®

DOI: 10.1249/MSS.0000000000000615

Most studies that measure plantar pressure report discrete variables such as peak and mean pressures for large areas, or "masks," under the foot (5,8,23,24,26). This is because the analysis techniques used require discrete inputs. Although a discrete approach is useful for reducing the dimensionality of a data set, it neglects the high resolution of the foot's sensory receptors. Consequently, the use of "masks" may result in overlooking important information such as subtle variations of the pressure distribution across the entire foot over time. Such subtle variations in the pressure distribution may be clinically important because they can directly affect the design features of a prescribed orthotic, such as identifying the exact location of required support (e.g., medial or lateral heel, posterior or anterior midfoot).

This article proposes a new technique that combines a principal component analysis (PCA) and a support vector machine (SVM), pattern recognition techniques that have the power to extract important information from comprehensive data sets. PCA allows for the extraction of correlated submovements, called principal components (PC) or features (11). The first few PC account for the most variability in the data set and are commonly associated with important and dominant aspects of the total movement. Although PCA has been used in human movement studies to identify features of gait (6,16,28), this study is the first to extract the principal features of loading at the foot from plantar pressure data. PCA can be used to visualize and interpret differences in loading across footwear conditions. In addition, it is used to reduce the dimensionality of a data set to its most important information for enhanced ability to classify footwear interventions. Data classification tools such as SVM have recently been used to classify different groups using the features obtained from PCA analysis (10,28). Combining PCA and SVM as comprehensive analysis approaches yields the possibility of gaining knowledge about the specificities of different footwear conditions.

Therefore, this article's objective was to develop and use a comprehensive technique for assessing the effects of different footwear interventions on plantar loading. To test the effectiveness of this new approach, three different footwear conditions that represented three popular running shoe categories and that possessed distinct differences in their mid- and outer sole constructions were selected. The three conditions were one standard cushioned shoe with a thick midsole, one racing flat with a thin midsole, and one minimalist shoe condition that mimicked the barefoot condition (e.g., rounded heel and conforming midfoot). The following four hypotheses were investigated:

1. Mean pressure patterns will appear different across running shoes that differ in their construction.
2. Using PCA, distinct loading features will be identified to provide enhanced functional interpretation of plantar loading during running.
3. Using these features as inputs to an SVM will allow for successful classification of different shoe conditions.
4. The discriminant that allows classification across shoe conditions will reveal differences in the plantar pressure distributions among shoes.

The analysis approach proposed in this study provides detailed information about the relation between shoe sole construction and plantar pressure loading that is often not captured in traditional approaches. The proposed approach allows for extraction of precise information about whether observed differences in plantar pressure variations between shoes are meaningful. If differences determined through the proposed analysis are found to be meaningful, shoe manufacturers and testers will know that the plantar distribution is significantly affected, which may then provide information about the effects that a shoe has on more proximal joint kinematics and loading.

METHODS

Participants and Measurement Protocol

Forty-two participants (21 men and 21 women), mean (± SD) age of 30.2 ± 9.8 yr, participated in this study. Participants were healthy and physically active recreational runners (≥2 runs per week) with no lower extremity pain or injuries at the time of testing. Participants were self-described heel strikers. The heel striking technique was confirmed from observation during testing and from the plantar pressure data. All participants provided written informed consent before the start of data collection according to the policy on research using human subjects of the institution's research ethics board.

Participants warmed up by walking on a treadmill for 2 min and completing four overground running practice trials in the laboratory before beginning data collection. Participants then completed 10 overground running trials on an indoor runway approximately 30 m in length in each of the three shoe conditions (Fig. 1). All participants were running at the same speed of 3.33 ± 0.50 $m \cdot s^{-1}$, which was monitored using timing lights positioned 1.9 m apart in the center of the runway. The order in which participants ran in each shoe condition was randomized across participants.

Shoe Conditions

The three running shoes varied in their construction features (Fig. 1) and material properties (Table 1). Shoe A was the Mizuno BE, a minimalist shoe with a thin outer sole construction, a molded insole, and a curved heel pad. Shoe B was the Mizuno Wave Rider, a standard "cushioned" running shoe with a thick outer sole and a middle groove on the outer sole at the heel. Shoe B possessed the thickest midsole out of the three shoe conditions. Shoe C was the Mizuno Wave Universe, a very light racing flat with a thin outer sole. Shoe C also had a distinct middle groove on its outer sole heel. The masses of the men's US size 9 shoes were 193, 270, and 112 g, for shoes A, B, and C, respectively.

FIGURE 1—Shoe conditions. A, Shoe A, Mizuno BE, a minimalist shoe with a rounded heel construction. B, Shoe B, Mizuno Wave Rider, a standard shoe with a cushioned midsole. C, Shoe C, Mizuno Wave Universe, a very light racing flat.

Measurement of Plantar Pressure Distribution

Pressure data from the left foot were recorded at a sampling frequency of 200 Hz using an instrumented insole (Pedar®-X; Novel, Germany). Appropriately sized calibrated insoles for each participant's shoe size were used. Insoles were 1.9 mm thick and allowed for collecting pressure data from 99 cells distributed across the sole. The fourth step of every running trial was analyzed, which corresponded to a step that occurred when the participant was running between the timing lights at a constant speed. Participants wore a small backpack containing a data logger box to which the insoles were connected via cables that were secured to the participant's leg using tape. The data were transmitted to an SD card in the data logger box and downloaded to a computer after the experiment.

Data Analysis

Data preprocessing and organization. The force of each of the 99 cells at each instant in time was calculated as the cell's pressure multiplied by its area. Force values of the 99 cells at each instant in time were organized into the shape of a foot as a 15 (row) × 7 (column) matrix (Fig. 2). Elements of the matrix that did not represent a cell were set to zero and did not contribute to the results. These 15 × 7 matrices were called "force-patterns." Force-patterns were reshaped into "force-vectors" by appending the 15 rows of the force-pattern to one another. The force data as collected

TABLE 1. Physical characteristics of each of the three shoe conditions.

	Shoe A	Shoe B	Shoe C
Midsole (EVA) hardness	Shore C, 70 ± 4C	Shore C, 55 ± 4C	Shore C, 56 ± 4C
Outer sole (rubber) hardness	Shore A, 60 ± 3C	Shore A, 70 ± 3A	Shore A, 70 ± 3A
Heel cushioning (G score)	22.7G	11.2G	19.4G
Heel outer sole groove width[a] (cm)	N/A	2.7	2.5
Heel outer sole groove distance from heel edge[a] (cm)	N/A	3.0	2.3

[a]For men's US size 9.

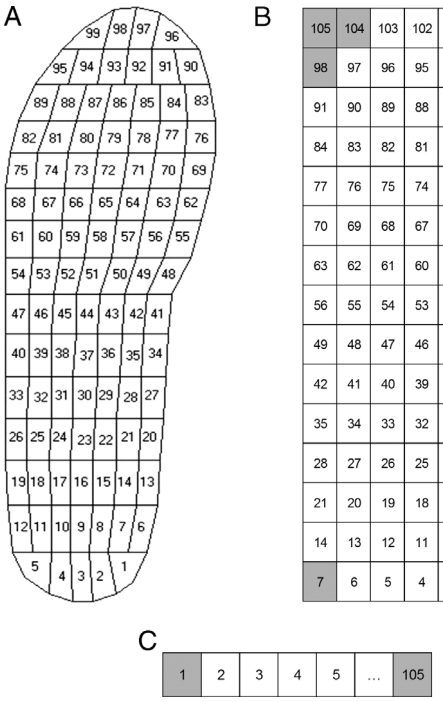

FIGURE 2—A, Cell matrix on the Pedar®-X insole. B, Force-pattern matrix. C, Force-vector. *Shaded areas* correspond to elements that were set to zero because they did not represent a cell. These elements did not contribute to the results.

from the Pedar system were not filtered. Instead, the data from each trial (i.e., step) were linearly interpolated to provide 100 time points indicating 1% intervals of the stance phase—a normalizing process that effectively smoothened the data. These data were then linearly interpolated to provide 100 time points for the step. For example, if one running step lasted 300 ms, this step was captured by 60 samples (because the sampling frequency was 200 Hz). There was one force-vector per time point, thus 100 force-vectors for each ground contact (i.e., trial). Therefore, the 10 trials (i.e., 10 steps) of a participant running in a given shoe condition yielded 1000 force-vectors. There were 42,000 force-vectors per shoe condition (i.e., 42 participants × 1000 force-vectors).

PCA. For each shoe, the mean force-vector of that shoe across trials and participants was first subtracted from the 42,000 force-vectors. Then, the new vectors were organized as rows forming a shoe-specific matrix. An input matrix was then created from the three stacked shoe-specific matrices, yielding a matrix with 126,000 rows and 105 columns (42000 × 3 and 15 × 7 cells) (i.e., axes of the coordinate system). A PCA was applied to this input matrix.

The outputs of the PCA are eigenvectors and eigenvalues of the covariance matrix of the input matrix. The eigenvectors, or PC, represent a new set of axes in the original vector space defined by the input matrix. Each one of these vectors represents a part of the variance of the input data set. The PC are numbered in descending order of the explained variance, which is indicated by the corresponding eigenvalues. Higher-ordered PC explain less of the total variance and are often thought of as noise. It is therefore common practice to reduce the number of PC to those that explain most of the variance. However, as shown in previous studies, differences between conditions, such as shoes, may not be found in the lower-ordered PC that represent most of the movement's variance (16). In the present analysis, we considered those PC that cumulatively accounted for 99% of the data's variance because this percentage of accounted variance provided plateau in the classification rates computed in the subsequent SVM analysis.

To include differences between the mean force vectors of each shoe condition in the classification procedure described in the following section, residual vectors that captured this information were calculated and added to the calculated PC. Indeed, these mean force-vectors cannot be represented by the axes of the PC space as calculated using the PCA given that the means were subtracted before computing the PCA. Therefore, additional, orthogonal, and residual vectors of the mean force-vectors were computed. To compute these vectors, the mean force-vector of the first shoe was first projected onto the PC. These projections were used to reconstruct the part of the mean force-vector that can be captured by the PC. Next, the reconstructed part of the mean force-vector was subtracted from the mean force-vector, yielding a residual vector that is orthogonal to the PC. This residual vector was added as an additional PC. The projections onto the PC allowed for full reconstruction of the mean force-vector of the first shoe. This procedure was then repeated for the mean force vector of the second and third shoes. Thus, three additional vectors were added to the set of PC, for a total of 38 PC.

The amount that each PC contributed to the force-vector was represented by the corresponding PC-weights. The PC-weights were computed as the projections of the force-vectors onto the PC. The PC-weights form a p-vector in PC-space, and each component of the p-vector represents the PC-weights of one force-vector. The p-vectors could then be transformed back, or reconstructed, into the original 105 cell vector-space to provide force-patterns described by each PC.

The stance phase was subdivided into 100 equidistant points representing time as a percentage of stance phase (t%). There was a p-vector for each of these points. For a given PC, the PC-weights were represented as a function of t% and shown as a waveform that indicated the contribution of one PC to the total force-pattern during the entire stance phase. Thus, positive and negative values in the waveform indicated whether the forces represented by the PC were added or subtracted to produce the total force. However, the overall reconstructed force will always only contain positive values.

Isolating shoe-specific differences for classification of trials. Pairwise differences across shoes were assessed using an SVM. The 100 p-vectors per trial (i.e., step) were appended to one another and formed one row of a matrix. For each of the three pairwise comparisons, the rows of the first shoe were stacked on top of those of the second shoe and together formed an 840 row (2 shoe conditions × 42 participants × 10 trials) and 3800 column input matrix for the SVM (38 PC × 100 time points). The SVM binomially classified the trials by identifying an optimal separating hyperplane that maximized the margin between the data from the two conditions (3).The SVM had two specific outcomes: 1) the quality of the differences in the force-pattern between shoe conditions and 2) the actual differences between the shoe conditions displayed as reconstructed force-patterns. The quality of the differences between shoes was assessed by a classification rate calculated using a leave-one-out cross-validation approach (16). The statistical significance of the classification rate was assessed using a binomial test, yielding a two-tailed p-value. The actual differences in the force-pattern between the shoe conditions were obtained using a linear kernel function. The linear kernel allowed computation of a unit vector normal to the separating hyperplane called the discriminant vector. From the discriminant vector, it was possible to obtain the spatiotemporal contribution of the cells of a force-pattern to the separation between two conditions. To express this force-pattern in the original data's units (i.e., body weight), the discriminant vector, which was calculated in the PC-vector space, was back-transformed into the 105-axis space of the original cell data. This allowed for functional analysis of where the differences laid over the foot between the conditions (25).

All data were processed and analyzed using Matlab software (version 2012b; The MathWorks, Natick, MA). The figures displaying force-patterns were created using the

Matlab function "contouf," which interpolated the mean force between the plantar pressure cells to provide smoother view of the force distribution across the foot. Although the force-patterns were best visualized as animations (attached to this article in Supplemental Digital Content format), the force-patterns were also displayed for three instances of *t*% during stance: 12%, 45%, and 75%. These instances were selected after pilot studies revealed that they provided the best visualization of the force-patterns representing three important phases of stance across all three shoes: heel impact, push-off, and toe-off.

RESULTS

Qualitative differences in force-patterns across shoe conditions. The mean force-patterns based on the raw force distribution data seemed different across shoe conditions (Fig. 3) (see Video, Supplemental Digital Content 1, Mean force distribution patterns for the three shoe conditions and total force across cells for each shoe (14 s, 12.7 MB), http://links.lww.com/MSS/A503. Shoe A displayed a central pressure point at the heel at 12% stance, whereas shoe C displayed dual pressure points at the heel, as follows: one medial and another lateral at the same time point. At 12% stance, shoe B displayed medial–lateral distribution of force. At push-off (45% stance), shoe B displayed more distributed force-pattern across the sole compared with the minimalist shoes (i.e., shoes A and C). Shoe A displayed the least amount of force at the instep of the foot at 45% stance. All shoe conditions displayed similar force distribution pattern at push-off (75% stance).

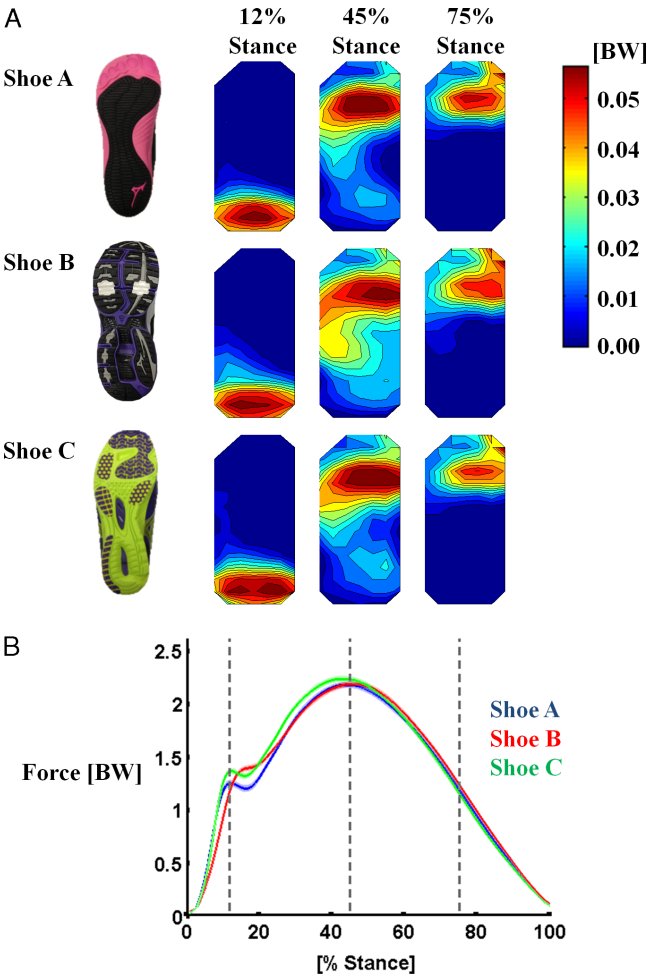

FIGURE 3—A, Mean force distribution patterns for the three shoe conditions at three instances of the stance phase of running, expressed relative to the mean ground reaction force, as follows: 12% stance (approximate heel impact peak), 45% stance (approximate active peak), 75% stance (approximate push-off). B, Total force across cells for each shoe.

Principal features of running. Results from the PCA revealed PC that represented distinct loading features at the foot during the stance phase of running. Thirty-five different PC were necessary to explain 99% of the variance in the data. The first PC accounted for 51% of the data's variance. As seen from the mean reconstructed force-pattern (Fig. 4A), the first PC represented the loading of the heel and unloading of the forefoot in early stance (12% stance), followed by the loading of the forefoot in mid-to-late (45%–75%) stance (Fig. 4A, top row). The second PC accounted for 23% of the data's variance. Each PC represents the variables (i.e., cells from the instrumented insole) correlated to one another as per the definition of PCA. Therefore, the second PC's force-pattern showed that the heel cells and lateral forefoot cells are correlated as their loading magnitude increased simultaneously (Fig. 4B). The third PC accounted for 6% of the data's variance and represented the correlated loading of the posterior heel and hallux (Fig. 4C) (see Video, Supplemental Digital Content 2, Mean reconstructed force- patterns for each PC and corresponding PC weights through time for each shoe (12 s, 18.7 MB), http://links.lww.com/MSS/A504.

Differences captured by the PC-weight waveforms. The mean PC-weights through time were different across shoes for all the PC (Fig. 4, bottom row) (Supplemental Digital Content 2, http://links.lww.com/MSS/A504). For the first PC, the PC-weights of both minimalist shoes (i.e., shoes A and C) were similar throughout stance, whereas the slope of the PC-weight waveform for shoe B was lower throughout midstance. For the second PC, the peak loadings after heel impact varied across shoes. Shoe C had the greatest impact peak, whereas shoe A had the lowest impact peak. Shoe B had an impact peak magnitude that fell between the other two shoes but had a substantially lower loading rate than both minimalist shoes. At midstance, both minimalist shoes had similar magnitudes, whereas the loading magnitude for shoe B was slightly lower. For the third PC, shoes A and C displayed similar magnitudes at 75% stance, but the weighting magnitude was substantially greater for shoe A between 15% and 45% stance. The weighting magnitude was lowest for shoe B compared with that for the two other shoes at 12%, 45%, and 75% stance. As per their mathematical definition, the sum of the force-patterns of all PC for each shoe (Fig. 4, top row) (Supplemental Digital Content 2, http://links.lww.com/MSS/A504) represented the total force-pattern (Figs. 3A and 4B and C) (Supplemental Digital Content 1, http://links.lww.com/MSS/A503) and the

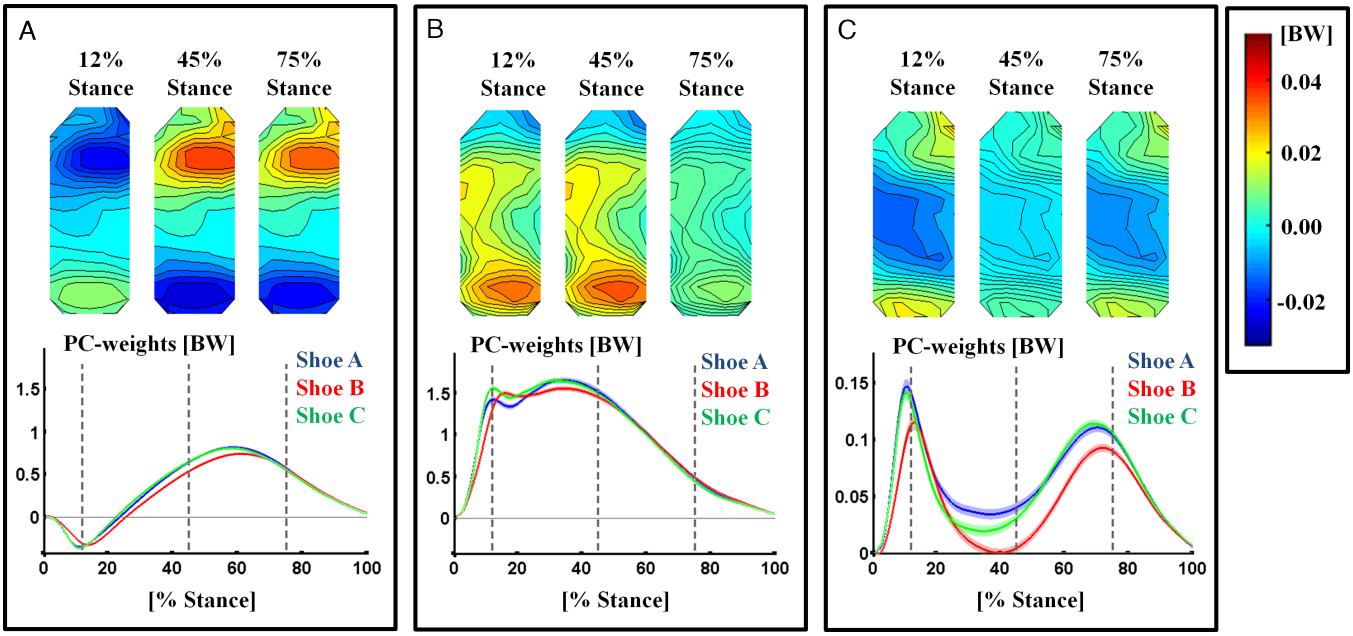

FIGURE 4—Mean reconstructed force-patterns at 12% of stance, 45% of stance, and 75% of stance (*top row*) and the corresponding mean (±SE) PC-weights through time for each shoe (*bottom row*) for each of the first three PC. Only one force-pattern is shown for each time point (*top row*) rather than three (for each shoe) because the force-pattern is the same for all shoes, with only the loading magnitudes being different across shoes.

sum of the PC-weights (Fig. 4, bottom row) (Supplemental Digital Content 1, http://links.lww.com/MSS/A503) of each shoe represented the total force for that shoe (Fig. 3D).

Quantification of differences across shoe conditions. Using the force-patterns projected on the first 35 PC and the three residual means for each shoe, the SVM analysis allowed for successful classification of all three pairwise shoe comparisons. The classification rate computed by the leave-one-out method was 98.25% for comparing shoes A and B, 99.21% for comparing shoes B and C, and 94.21% for comparing shoes A and C. All these classification rates were statistically highly significant ($P < 0.001$).

In addition to allowing for the classification of the shoe conditions, the SVM results also allowed for identifying where the conditions differed with one another with respect to the location of the loading under the foot. The location and timing of the load between shoes varied, according to the SVM discriminant, across each pairwise comparison (Fig. 5) (see Video, Supplemental Digital Content 3, Mean difference force-patterns obtained from the SVM discriminant vector (12 s, 22.2 MB), http://links.lww.com/MSS/A505). Differences between shoe A and B at 12% were due to a central pressure point at the heel for shoe A and greater force at the anterior aspect of the heel for shoe A (Fig. 5A). At 45% stance, differences between shoes A and B were due to greater force at the instep for shoe B and greater force at the forefoot for shoe A. Differences between shoes A and C at 12% were due to a central versus mediolateral pressure points for shoes A and C, respectively. At 45% stance, there was greater force at the instep for shoe C compared with that for shoe A and greater force at the center of the midfoot for shoe A. Differences between shoes B and C at 12% stance were due to greater force at the anteriolateral aspect of the heel for shoe B but greater force posterior to this region for shoe C. At 45% stance, differences due to shoe C were at the anterior aspect of the midfoot compared with the differences due to shoe B.

DISCUSSION

The purpose of this study was to develop and use a comprehensive technique for assessing the effects of different footwear interventions on plantar loading. From plantar pressure measurements across different shoe conditions during running, differences in force-patterns at the foot were obtained, and these differences were quantified using pattern recognition techniques. These provided a novel and enhanced way of assessing plantar loading across footwear interventions.

The force-patterns were different across the shoe conditions tested, which supports the first hypothesis. The differences identified in the loading patterns across the entire foot provided detailed and comprehensive information that may have been overlooked if the foot had been considered as larger masked areas. For example, the central pressure point at the heel in the force-pattern of shoe A at 12% stance (Fig. 3A) suggests that the foot has the freedom to pivot about the heel after impact. On the other hand, shoes B and C show mediolateral pressure distribution (Fig. 3A). This distribution may be a reflection of the groove present in shoes B and C's outer sole. This interpretation may be explained by less support directly underneath the outer sole groove (i.e., no direct contact with the ground), likely preventing force from being effectively transferred to the middle of the heel because of a lack of midsole plate stiffness. Instead, the medial–lateral heel supports on shoe B and C's outer sole provided force to the

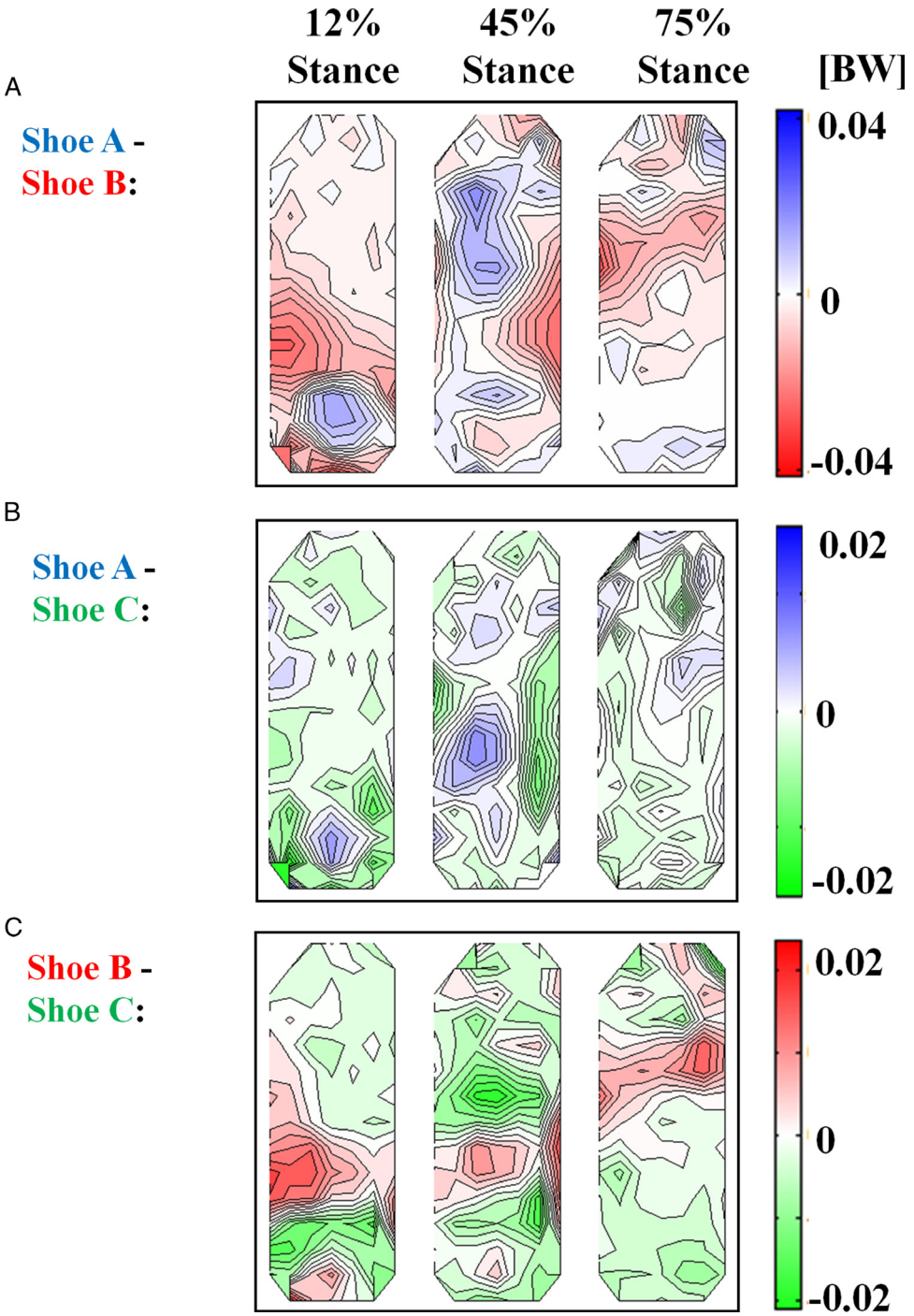

FIGURE 5—Mean difference force-patterns obtained from the SVM discriminant vector at 12% stance (*left column*), 45% of stance (*middle column*), and 75% of stance (*right column*). The discriminant was back-transformed to obtain the raw data's units.

medial and lateral aspects of the heel, which likely affords greater stability of these shoes in the frontal plane compared with shoe A, which possessed a rounded heel. The medial–lateral pressure distribution pattern was less pronounced for shoe B than for shoe C, which is consistent with previous findings reporting greater pressure distribution (and therefore less-defined reflection of the outer sole's construction features) for thicker midsoles (23,26). This information may be useful for shoe designers because it shows that manipulations to the outer sole design, especially in minimalistic shoes, can affect the plantar pressure during running. The potential to manipulate the force-patterns by altering the outer sole is important because differences in pressure patterns across the foot have been found to affect comfort (5).

The principal loading features, or PC, identified in this study provide enhanced and comprehensive information about the effect of different shoe constructions. This finding supports the second hypothesis. The two minimalist shoes

(i.e., shoes A and C) showed similar behaviors with respect to the shift of loading from the heel to the forefoot, as seen from the first PC-weights (Fig. 4A). However, these two shoes differed with respect to the second and third PC (Fig. 4B and C). PC2 captured the impact phase that is commonly interpreted from the vertical ground reaction force. It showed that shoe B, which possessed the thickest midsole, had the latest impact peak onset compared with the two minimalist shoes, which is consistent with results reported previously (27). PC3 provided information regarding the differences in loading between the heel/toes and the midfoot (Fig. 4C). The greater PC-weights for shoe A compared with those for the two other shoes at midstance indicated that the loading was less distributed across the length of the sole. This result may either be due to shoe A's hollow outer sole at the midfoot or may be an indication of shoe A's greater midsole stiffness.

The shoe conditions were classified successfully from a SVM, which supported our third hypothesis. The first three PC were sufficient to reveal some differences, but 35 PC and the residual means were needed to classify the shoes successfully. This result is consistent with a previous finding suggesting that the differences relevant to classification of the effect of different footwear are captured by higher-order PC (16). Differences that allow classification of the data can be found in the SVM discriminant.

The difference patterns computed from the SVM reveal in great detail where the differences occurred (Fig. 5) (Supplemental Digital Content 3, http://links.lww.com/MSS/A505). For example, the observation that Figure 5A and C look similar indicates that the reason may be explained from properties of shoe B, which had thicker midsole than the other shoes. In both these plots, shoe B had greater loading at the lateral aspect of the foot at 12% stance and at the forefoot at 75% stance. This may be due to a more distributed force pattern compared with that for the minimalist shoes. In addition, the low loading at the instep of shoe A observed from the mean force distribution patterns (Fig. 3A) is reflected in both mean difference force-patterns involving shoe A (Fig. 5A and C). This was likely due to shoe A's thin midfoot outer sole. The result that the magnitude scale in the difference plots was greatest for the comparison of shoe A vs. shoe B (Fig. 5A) is likely a consequence of shoes A and B being the most different in their construction, with shoe A having a rounded (as opposed to flat) heel and thinner midsole than shoe B. These differences in force-patterns could be used to modify shoe construction properties to specific requirements. For example, a shoe that is modified in a single aspect of its design (e.g., upper or lacing design) may be compared with the original shoe using the proposed method to ensure that the force-pattern remains the same. Such a technique would allow focusing on distinct design features while ensuring that comfort or performance, which might be due to loading patterns, is not compromised.

This study's methodology and results have important practical applications. One such application is that it would not be relevant for a user to select a shoe or for a manufacturer to alter a shoe's construction if the classification rate from the SVM would not be significant. Because the differences identified are shoe specific, they can be used to select a shoe that fulfills the requirements of a user. The PC described here are not properties of the individual runners but are rather properties imposed by a specific shoe. However, alternative approaches based on the proposed methodology may enable comparison across individuals or groups of individuals. An alternative approach would be to extract the principal loading features of a single person. This approach could be advantageous in a clinical setting where a similar analysis as proposed in this study could be used in understanding how different footwear constructions could help neuropathic patients prevent foot ulcers (12,22). In addition, a similar classification method to the one proposed here could be used as a diagnosis and/or rehabilitation monitoring tool. Using the classification method, neuropathic populations could, for instance, be identified (i.e., classified vs healthy individuals) with high accuracy, and interventions can then be provided to reduce harm on the musculoskeletal system. Similarly, groups of individuals who respond similarly to a given intervention or motor task, such as overpronators, could be classified according to characteristic force-patterns.

There are limitations to the methods of this study. First, one must be careful in interpreting the PC-weights from each PC because they are not independent from one another. For example, the PC-weights from PC1 are negative at heel strike (Fig. 4A) and then become positive at push-off. The negative loading cannot be interpreted without considering the fact that the PC-weights from other PC contribute positively to the loading at heel strike, summing to positive total force at heel strike. Second, the functional interpretations of the force-patterns from the reconstructions of each PC are subjective. PCA outputs PC that represent correlated aspects of the data that contribute most of the data set's variance. These features must then be given a context using the reconstructed force-patterns and the PC-weights. For example, because the PCA does not define the sign of the PC, PC1 in this study can be represented in two ways, as follows: as the loading of the heel followed by the loading at the forefoot or as the unloading of the forefoot followed by the loading of the forefoot. Third, this study aimed to describe the mean effect of different shoe constructions for many individuals. Therefore, the results do not consider the varying effects across different groups of individuals. In the current study, participants were not screened for any abnormalities or foot conditions that may have resulted in them being outliers. Fourth, the 3-mm instrumented insole added padding to the shoe insoles and potentially reduced the effect of the shoe outer sole constructions on the loading at the foot. Thus, in reality, the observed effects may be even more pronounced. In addition, the cables attached to the participants' legs and the backpack containing the data logger box may have affected the participants' gait. However, these factors were consistent across shoes and therefore likely represent a bias toward the null (i.e., no difference across shoe conditions).

In conclusion, the results demonstrated that correlated loading features (PC) can be extracted from plantar pressure data during running using PCA. The first three PC of plantar pressure described the loading shift from the heel to the forefoot, the loading of the heel and lateral forefoot, and the loading of the tip of the heel and hallux. The PC-weights for each PC allowed for identification of differences and function interpretations of the effects across all three shoe conditions. An SVM was then used to include the information of higher-order PC. This allowed classification of shoe conditions and identification of the relevant locations of loading differences on the foot due to the shoes. These locations are found by the algorithm and differ very much from locations selected by researchers on the basis of informed assumptions. These results provide very detailed information that allows for interpreting changes in plantar pressure caused by different shoe constructions. A similar analysis technique may be used in the future to assess the effects of different footwear or to compare or diagnose (i.e., classify) different groups of individuals (e.g., in a clinical environment) on the basis of plantar pressure data.

This study was funded by Mizuno Corporation (Osaka, Japan), and Biomechanigg Sport and Health Research (Calgary, Canada). The authors would like to acknowledge Sandro Nigg from the University of Calgary for his contribution to the study design and experimental protocol as well as Takao Oda and Yasunori Kaneko, from Mizuno Corporation, for their collaboration and feedback on the results.

Mizuno Corporation (Osaka, Japan) funded this research and also provided the shoes that were used in the testing. However, the results presented in this article do not in any way represent a bias toward Mizuno products over other brands.

The results of the present study do not constitute endorsement by the American College of Sports Medicine.

REFERENCES

1. Alfuth M, Rosenbaum D. Long distance running and acute effects on plantar foot sensitivity and plantar foot loading. *Neurosci Lett*. 2011;503(1):58–62.
2. Baltich J, Maurer C, Nigg B. Increased dynamic joint stiffness and peak vertical impact forces with softer shoe midsoles. *Footwear Sci*. 2013;5:S12–3.
3. Begg R, Kamruzzaman J. A machine learning approach for automated recognition of movement patterns using basic, kinetic and kinematic gait data. *J Biomech*. 2005;38(3):401–8.
4. Cavanagh P, Hewitt F, Perry J. In-shoe plantar pressure measurement: a review. *Foot*. 1992;2(4):185–94.
5. Chen H, Nigg BM, Hulliger M, de Koning J. Influence of sensory input on plantar pressure distribution. *Clin Biomech (Bristol, Avon)*. 1995;10(5):271–4.
6. Daffertshofer A, Lamoth CJ, Meijer OG, Beek PJ. PCA in studying coordination and variability: a tutorial. *Clin Biomech (Bristol, Avon)*. 2004;19(4):415–28.
7. De Wit B, De Clercq D, Lenoir M. The effect of varying midsole hardness on impact forces and foot motion during foot contact in running. *J Appl Biomech*. 1995;11(4):395–406.
8. Dixon SJ. Use of pressure insoles to compare in-shoe loading for modern running shoes. *Ergonomics*. 2008;51(10):1503–14.
9. Eils E, Nolte S, Tewes M, Thorwesten L, Volker K, Rosenbaum D. Modified pressure distribution patterns in walking following reduction of plantar sensation. *J Biomech*. 2002;35(10):1307–13.
10. Eskofier BM, Federolf P, Kugler PF, Nigg BM. Marker-based classification of young-elderly gait pattern differences via direct PCA feature extraction and SVMs. *Comput Methods Biomech Biomed Engin*. 2013;16(4):435–42.
11. Federolf P, Reid R, Gilgien M, Haugen P, Smith G. The application of principal component analysis to quantify technique in sports. *Scand J Med Sci Sports*. 2014;24(3):491–9.
12. Fernando ME, Crowther RG, Pappas E, et al. Plantar pressure in diabetic peripheral neuropathy patients with active foot ulceration, previous ulceration and no history of ulceration: a meta-analysis of observational studies. *PLoS One*. 2014;9(6):e99050.
13. Goldberg DA, Whitesel DL. Heel counter stabilization of the running shoe. *J Orthop Sports Phys Ther*. 1983;5(2):82–3.
14. Jordan C, Payton C, Bartlett R. Perceived comfort and pressure distribution in casual footwear. *Clin Biomech (Bristol, Avon)*. 1997;12(3):S5.
15. Kavounoudias A, Roll R, Roll JP. The plantar sole is a 'dynamometric map' for human balance control. *Neuroreport*. 1998;9(14):3247–52.
16. Maurer C, Federolf P, von Tscharner V, Stirling L, Nigg BM. Discrimination of gender-, speed-, and shoe-dependent movement patterns in runners using full-body kinematics. *Gait Posture*. 2012;36(1):40–5.
17. McKeon PO, Hertel J, Bramble D, Davis I. The foot core system: a new paradigm for understanding intrinsic foot muscle function. *Br J Sports Med*. 2015;49(5):290.
18. Nigg BM. *Biomechanics of Sport Shoes*. 1st ed. Calgary (Canada): Topline Printing, Inc; 2010. p. 300.
19. Nigg BM, Bahlsen HA, Luethi SM, Stokes S. The influence of running velocity and midsole hardness on external impact forces in heel-toe running. *J Biomech*. 1987;20(10):951–9.
20. Nurse MA, Hulliger M, Wakeling JM, Nigg BM, Stefanyshyn DJ. Changing the texture of footwear can alter gait patterns. *J Electromyogr Kinesiol*. 2005;15(5):496–506.
21. Orth D, Davids K, Wheat J, et al. The role of textured material in supporting perceptual-motor functions. *PLoS One*. 2013; 8(4):e60349.
22. Owings TM, Apelqvist J, Stenstrom A, et al. Plantar pressures in diabetic patients with foot ulcers which have remained healed. *Diabet Med*. 2009;26(11):1141–6.
23. Queen RM, Abbey AN, Wiegerinck JI, Yoder JC, Nunley JA. Effect of shoe type on plantar pressure: a gender comparison. *Gait Posture*. 2010;31(1):18–22.
24. Sobhani S, van den Heuvel E, Bredeweg S, et al. Effect of rocker shoes on plantar pressure pattern in healthy female runners. *Gait Posture*. 2014;39(3):920–5.
25. Stirling LM, von Tscharner V, Kugler PF, Nigg BM. Classification of muscle activity based on effort level during constant pace running. *J Electromyogr Kinesiol*. 2011;21(4):566–71.
26. Wiegerinck JI, Boyd J, Yoder JC, Abbey AN, Nunley JA, Queen RM. Differences in plantar loading between training shoes and racing flats at a self-selected running speed. *Gait Posture*. 2009;29(3):514–9.
27. Willy RW, Davis IS. Kinematic and kinetic comparison of running in standard and minimalist shoes. *Med Sci Sports Exerc*. 2014; 46(2):318–23.
28. Wu J, Wang J. PCA-based SVM for automatic recognition of gait patterns. *J Appl Biomech*. 2008;24(1):83–7.